A Global Decentralized Control Strategy for Urban Vehicle Platooning using Monocular Vision and a Laser Rangefinder

P. Avanzini, E. Royer, B. Thuilot and P. Martinet
LASMEA - 24 avenue des Landais - 63177 Aubière - FRANCE
Pierre.AVANZINI@lasmea.univ-bpclermont.fr

***Abstract*—To address traffic saturation in cities, new "Urban Transportation Systems", based on electric vehicles in free-access, are in developing. One necessary functionality of such systems is their ability to move in a platoon fashion. A global decentralized platoon control strategy, supported by inter-vehicle communications, is addressed in this paper, relying on nonlinear control techniques. The main interest in a global approach is that servoing error accumulation can be avoided, whatever the platoon length. However, absolute vehicle localization is then required. In urban applications, cameras are realistic sensors, but localization is supplied in a 3D visual virtual world, slightly distorted w.r.t. the actual metric one. To enable accurate guidance, local corrections to the visual world are here computed from the data supplied by a laser rangefinder mounted on the second vehicle, and then shared with the whole platoon. Full-scale experiments demonstrate the performance of the proposed approach.**

***Index Terms*—mobile robots, nonlinear control, platooning, automatic guided vehicles, monocular vision, laser rangefinder.**

I. Introduction

In order to reduce nuisances linked to the saturated traffic, new "Urban Transportation Systems" are in developing. Some projects, based on urban vehicles in free access, have been investigated since the mid-90's, e.g. Praxitèle in France [3]-[7], CarLink in the USA [11], Crayon in Japan [5]. Fully automated navigation for such vehicles is presently extensively discussed. One functionality of special interest is automated vehicle platooning, since cooperative navigation can ensure more coherent motions within the city, leading to an increase in traffic as well as an enhancement in safety. In addition, this functionality allows to easily adapt the transport offer (via platoon length) to the actual need, and maintenance is also facilitated by the possibility of leading manually the way to other vehicles. Platooning is therefore considered in this paper.

Different approaches can be proposed. Some applications, such as the majority of Automated Highways Systems, need an equipped road with an adapted architecture as described, for instance, in PATH project [6]. Unluckily, the cost of implementing the infrastructure and the fact that these systems cannot be used outside of the equipped area appear as major constraints. Other alternatives can be classified according to the information used for vehicle control. The most standard approaches rely on local strategies, i.e. each vehicle is controlled from the data received from the single immediate front vehicle. For instance, visual tracking of the preceding vehicle has been proposed in [1], and generic control laws for tracking maneuvers have been designed in [13]. However, in the latter case, inter-vehicle communications are highly desirable, in order to access to the numerous required state variables with enough accuracy. Such local approaches present nevertheless some drawbacks. The most concerning one is error accumulation: the servoing errors, introduced by sensor noises, are necessarily growing from the first vehicle to the last one, leading to unacceptable oscillations. Such problems can be overcome by considering global strategies, i.e. each vehicle is now controlled from the data received from all vehicles, collected from appropriate communication channels. For instance, in [2], a global control strategy has been proposed, relying on an RTK GPS sensor for vehicle localization and on WiFi technology for inter-vehicle communication.

However, GPS is not the most appropriate sensor for urban navigation: low cost GPS receivers are not accurate enough with respect to this application, when RTK GPS are suitable, but very expensive and the satellite signals can be masked by tall buildings in urban canyons. In contrast, cameras appear as very attractive sensors in such situations: inner-city buildings offer a rich environment from an image processing point of view and cameras are quite cheap sensors. The difficulty is that absolute localization that can be obtained from such sensors is expressed in a visual virtual world, slightly distorted with respect to the actual metric world. Such deformations alter noticeably the estimation of inter-vehicle distances, and therefore impair longitudinal control performances.

It is shown in this paper that high accurate vehicle platooning can nevertheless be achieved if the visual virtual world is just supplemented with some local corrections. These latter are here derived from the telemetric data supplied by the laser rangefinder mounted on the second vehicle, and then shared with the whole platoon. This device introduces no additional cost, since anyway it is required for pedestrian supervision. More precisely, the paper is organized as follows: the global decentralized control strategy is first sketched in Section II. Then, principle and performances of absolute localization via monocular vision are discussed in Section III. Next, the local correction to the visual virtual world is presented in Section IV. Finally, experimental results are reported in Section V.

978–1–4244–2287–6/08/$25.00

II. Global decentralized control strategy

A. Modeling assumptions

Urban vehicles are supposed to move at quite low speed on asphalted roads. Dynamic effects can therefore be neglected: as corroborated by extensive tests performed in various situations (different masses onboarded, on sloping grounds, etc.) with our experimental vehicles shown in Figure 1, kinematic models can satisfactorily describe the behavior of such vehicles.

Fig. 1. Experimental vehicles: a Cycab leading a RobuCab

More precisely, in this paper, the celebrated tricycle model is considered: the two actual front wheels are replaced by a unique virtual wheel located at the mid-distance between the actual wheels. The notations are illustrated in Figure 2.

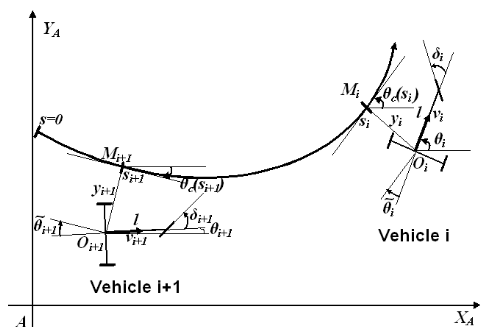

Fig. 2. Tricycle model description

- T : common reference path for any vehicle within the platoon, defined in an absolute frame $[A, X_A, Y_A)$
- O_i : center of the i^{th} vehicle rear axle
- M_i : closest point on T to O_i
- s_i : curvilinear coordinate of point M_i along T. It corresponds to the distance covered along T by vehicle i.
- $c(s_i)$: curvature of path T at M_i
- $\theta_c(s_i)$: angle of the tangent to T at M_i w.r.t. $[A, X_A, Y_A)$
- θ_i : heading of i^{th} vehicle at point O_i w.r.t. $[A, X_A, Y_A)$
- $\tilde{\theta}_i = \theta_i - \theta_c(s_i)$: angular deviation of i^{th} vehicle w.r.t. T
- y_i : lateral deviation of the i^{th} vehicle w.r.t. T
- δ_i : i^{th} vehicle front wheel steering angle
- l : vehicle wheelbase
- v_i : i^{th} vehicle linear velocity at point O_i
- n : number of vehicles in the platoon, i.e. $i \leq n$

B. Vehicle state space model

The configuration of the i^{th} vehicle can be described without ambiguity by the state vector $(s_i,\, y_i,\, \tilde{\theta}_i)$. The current value of these 3 variables can be inferred on-line by comparing vehicle absolute localization to the reference path. It can then be shown (see e.g. [10]) that tricycle state space model is :

$$\begin{cases} \dot{s}_i = v_i \, \frac{\cos\tilde{\theta}_i}{1 - y_i\, c(s_i)} \\ \dot{y}_i = v_i \, \sin\tilde{\theta}_i \\ \dot{\tilde{\theta}}_i = v_i \left(\frac{\tan\delta_i}{l} - \frac{c(s_i)\, \cos\tilde{\theta}_i}{1 - y_i\, c(s_i)} \right) \end{cases} \tag{1}$$

Platooning objectives can then be described as ensuring the convergence of y_i and $\tilde{\theta}_i$ to zero, by means of δ_i, and maintaining the gap between two successive vehicles to a fixed value d, by means of v_i. It is considered that $y_i \neq \frac{1}{c(s_i)}$ (i.e. vehicles are never on the reference path curvature center). In practical situations, if the n vehicles are well initialized, this singularity in equations (1) is never met.

C. Control law design

In previous work [2], it has been shown that exact linearization techniques offer a relevant framework to address platoon control: tricycle equations (1), as most of kinematic models of mobile robots, can be converted in an exact way into a so-called chained form, see e.g. [4]. Such a conversion is very attractive, since the structure of chained form equations allows to address independently lateral and longitudinal control.

Steering control laws δ_i can first be designed to achieve the lateral guidance of each vehicle within the platoon. In these control laws, v_i just appears as a free parameter. Since conversion of equations (1) into chained form is exact, all non-linearities can explicitly be taken into account. High tracking performances can then be ensured, whatever initial errors or reference path curvature. Details and performances of lateral control laws can be found in [12].

Control variables v_i can then be designed to achieve longitudinal control. In previous work [2], two longitudinal errors are considered:

$$\text{global error:} \quad e_i^1 \quad = s_1 - s_i - (i-1)\, d \tag{2}$$

$$\text{local error:} \quad e_i^{i-1} \quad = s_{i-1} - s_i - d \tag{3}$$

Both errors are curvilinear inter-distances: they are computed according to the distance actually covered by the vehicles (when lateral errors are close to zero) and therefore remain perfectly consistent, whatever reference path curvature (in contrast with euclidian inter-distances). More precisely, the global error e_i^1 and the local one e_i^{i-1} describe the longitudinal errors of the i^{th} vehicle with respect to the leader and to the preceding vehicle, see (2)-(3). It is clearly advantageous to design longitudinal velocities v_i in order to control e_i^1 rather than e_i^{i-1}: in the former case, for all the vehicles, the longitudinal error is computed with respect to a common index (i.e. the location of the leader), no error accumulation can therefore occur. The undesired oscillations that are noticed when e_i^{i-1} is controlled (in this case, since each vehicle is solely controlled with respect to the preceding one, the errors due to sensor noises are inevitably accumulated along the platoon) can then be avoided. Nevertheless, for obvious safety reasons, longitudinal laws cannot completely ignore the local error e_i^{i-1} (for instance, when a vehicle is abnormally approaching the preceding one). Therefore, in previous work [2], the longitudinal law is designed to control a composite error:

$$\begin{array}{rl}\text{composite} & \\ \text{error :} \quad x_i & = \sigma(e_i^{i-1})\, e_i^1 + \big(1 - \sigma(e_i^{i-1})\big)\; e_i^{i-1}\end{array} \tag{4}$$

$\sigma(.)$ is a smooth commutation function, giving the predominance, either to the global error e_i^1, when e_i^{i-1} is superior to some security distance (in this case, $\sigma(e_i^{i-1}) \approx 1$), or to the local error e_i^{i-1}, when it comes close to the security distance (in this case, $\sigma(e_i^{i-1}) \approx 0$). The overall longitudinal control scheme is shown in Figure 3.

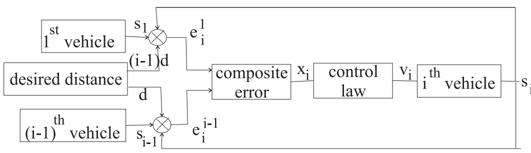

Fig. 3. Overall longitudinal control scheme

Exact linearization techniques can still be used to design velocity laws v_i: once more, nonlinearities in equations (1) can be explicitly accounted, and high accurate regulation of x_i to 0 can therefore be achieved. Experimental results, carried out with Cycab and RobuCab vehicles (see Figure 1), relying on RTK GPS for vehicle localization and WiFi technology for inter-vehicle communications, are reported in [2] and show the efficiency of the proposed global decentralized control strategy.

III. Localization with monocular vision

The implementation of the platooning control laws presented in previous section requires that some sensors can provide each vehicle with its absolute localization, in a common reference frame (in order that the composite errors x_i could be evaluated). RTK GPS receivers can supply such a localization, with a very high accuracy (± 2 cm). They have successively been used in [2]. However, they are quite expensive sensors, and above all they are not appropriate to urban environments, since satellite signals are likely to be frequently masked by tall buildings. In previous work [8], absolute localization from monocular vision has been alternatively proposed, and satisfactory accurate lateral guidance of a sole vehicle along a previously known reference path has been demonstrated. An overview of the localization approach is first sketched in Section III-A, and its limitations with respect to platooning applications are then discussed in Section III-B.

A. Localization overview

The localization algorithm relies on two steps, as shown in Figure 4. First, the vehicle is driven manually along the desired trajectory and a monocular video sequence is recorded with the on-board camera. From this sequence, a 3D reconstruction of the environment in the vicinity of the trajectory is computed. Because only one camera is used, this is a structure from motion problem well known in the computer vision community. The computation of the reconstruction is done off-line with a method relying on bundle adjustment. The trajectory is thus referred in a non-metric visual virtual world. However, the total covered distance supplied by on-board odometers, when compared to the same quantity evaluated from vision algorithms, enables to propose a global scale factor such that this visual virtual world is nevertheless close to the actual metric world.

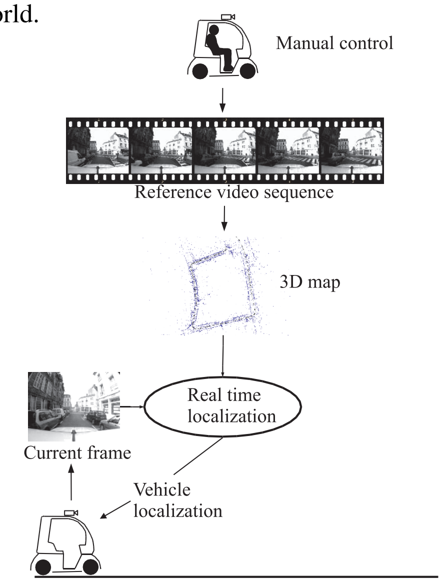

Fig. 4. Localization with monocular vision

The second step is the real time localization process. Interest points are detected in the current image. These features are matched with the features stored in the visual memory as part of the 3D reconstruction. From the correspondences between 2D points in the current frame and 3D points in the visual memory, the complete pose (6 degrees of freedom) of the camera is computed. Then, the pose of the vehicle on the ground plane (with only 3 degrees of freedom) is deduced, and finally the vehicle state vector $(s_i, y_i, \tilde{\theta}_i)$ and the curvature $c(s_i)$ required in control laws can all be inferred. More details and localization performances can be found in [9].

B. Distorsions in the visual virtual world

Platoon control in urban environment requires vehicle localization to be accurate to within some centimeters. The global scale factor computed from odometric data cannot guarantee such an accuracy: first, odometers cannot supply a covered distance accurate to within some centimeters when the reference trajectory length comes up to few hundred meters. Secondly, the distorsions between the two worlds are alas varying along the trajectory, as it can be observed in Table I: curvilinear lengths of 7 parts of a U-trajectory, denoted $[p_k,\, p_{k+1}]_{k\le 7}$, have been computed according to vision algorithms and to RTK-GPS measurements. The U-trajectory and the location of p_k points in the visual virtual world and in the metric one (as supplied by the RTK-GPS sensor) are shown respectively in Figures 5 and 6. It can clearly be noticed in Table I that the scale factor between the two worlds is not a constant.

These distorsions in the visual world are not a concern as long as only lateral guidance is considered: since the sign of the lateral and angular deviations y_i and $\tilde{\theta}_i$ supplied by vision

selected part	vision curvilinear length	rtk-gps curvilinear length	scale factor
$[\,p_1, p_2\,]$	31.9623 m	29.5015 m	0.9230
$[\,p_2, p_3\,]$	30.4699 m	27.7970 m	0.9123
$[\,p_3, p_4\,]$	31.9183 m	30.2179 m	0.9467
$[\,p_4, p_5\,]$	38.7124 m	37.3587 m	0.9650
$[\,p_5, p_6\,]$	32.0024 m	30.4700 m	0.9521
$[\,p_6, p_7\,]$	29.3850 m	30.4800 m	1.0373
$[\,p_7, p_8\,]$	34.9721 m	37.1272 m	1.0616

TABLE I
CURVILINEAR DISTANCE COMPARISON

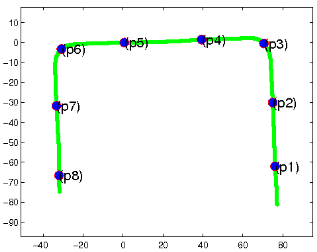

Fig. 5. Vision based trajectory

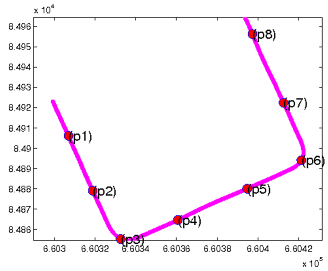

Fig. 6. RTK-GPS based trajectory

algorithms is always correct, these distorsions act only as control gain modifications. Asymptotic convergence of y_i and $\tilde{\theta}_i$ to 0 is therefore always guaranteed, and very satisfactory path following results can be obtained, as reported in [8].

The situation is different when longitudinal control is addressed: the distorsions in the visual world lead to inaccurate inter-vehicle distance evaluation, and therefore poor longitudinal control performances with respect to the metric world.

However, the experimental results reported in Figure 7 show that these distorsions are repeatable: lateral guidance along a 85m-long straight line has been performed four times. It can be noticed that the difference between the curvilinear abscissa supplied by vision algorithms and by the RTK-GPS sensor presents always the same changes along the trajectory. It appears therefore that the visual world and the metric one could fit if a set of local scale factors was used, instead of a sole global one. It is shown in the sequel that such an approach can significantly improve platooning control performances, and deliver the accuracy expected in urban environments.

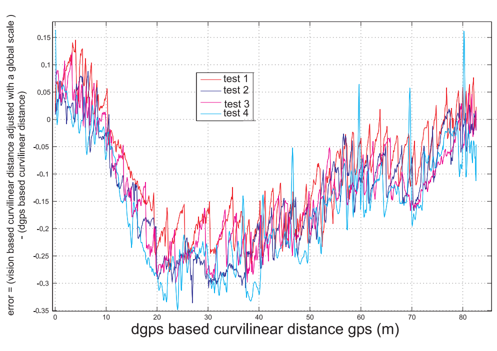

Fig. 7. Error in curvilinear evaluation during 4 straight line following

IV. CURVILINEAR DISTANCE ESTIMATION

Local scale factor estimation requires that some distances in the visual world could also be accurately evaluated in the actual metric one. Since RTK-GPS are not reliable sensors in urban environments and odometers are not accurate enough, it is here proposed to rely on laser rangefinders: these devices can provide very accurate measurements, and moreover introduce no additional cost, since they are already mounted on vehicles for pedestrian supervision. More precisely, local scale factors are here derived exclusively from the telemetric data supplied by the laser rangefinder of the 2^{nd} vehicle. These local corrections are then shared with the whole platoon via inter-vehicle communication for immediate use (the other vehicles do not have to rely on their own laser rangefinder) and also stored for subsequent uses: anytime the same trajectory has to be followed, platoon control can rely on the previously recorded local corrections, without further need of laser rangefinders (except of course for pedestrian supervision). The 3-steps procedure providing these local scale factors is now described.

A. Measured scale factor

First, the back of the leading vehicle is isolated in the telemetric data read by the second vehicle: depending on the type of the leading vehicle (i.e. Cycab or RobuCab, see Figure 1), an ellipse or a straight line is searched. Next, least square fitting is used to compute the pose of this pattern. The location of the rear axle center of the leading vehicle, shown in red in Figures 8 and 9, can then be inferred.

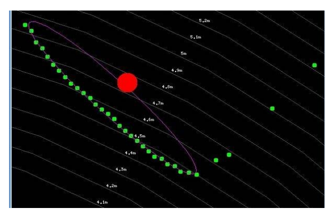

Fig. 8. Cycab in telemetric data

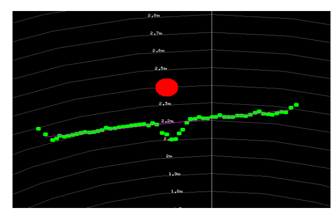

Fig. 9. RobuCab in telemetric data

Finally, a measured scale factor λ_m can be computed as the ratio between the euclidian inter-vehicle distance supplied by the laser rangefinder (expressed in the actual metric world) and the same quantity deduced from the state vectors of the leader and 2^{nd} vehicle, provided by vision algorithms, and transmitted via inter-vehicle communications. If O_l and O_f denote the rear axle center of respectively the leader and the 2^{nd} vehicle, then:

$$\lambda_m = \frac{\|O_l - O_f\|_{laser}}{\|O_l - O_f\|_{vision}} \tag{5}$$

B. Correction of the curvilinear abscissa

In order to present the second step of the procedure, let us consider the location of the leader and 2^{nd} vehicle at two successive instants, denoted t_1 and t_2 in Figure 10.

Let us also distinguish the two following curvilinear abscissas:

- s: raw curvilinear abscissa supplied by vision algorithms.
- $\hat{s}$: curvilinear abscissa corrected according to the local scale factors. $\hat{s}$ is therefore supposed to be expressed in the metric world.

Finally, let s_l^1 and s_l^2 *(resp.* s_f^1 *and* s_f^2*)* denote the raw curvilinear abscissas of the leader vehicle *(resp. the* 2^{nd} *vehicle)* at time t_1 and t_2. The same superscripts and subscripts are also used with the corrected curvilinear abscissa $\hat{s}$.

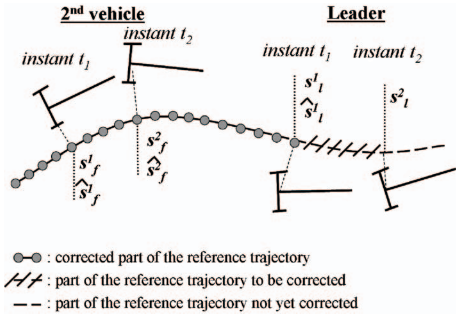

Fig. 10. Correction of curvilinear abscissa

Let us suppose that, relying on data up to time t_1, the curvilinear abscissa has been corrected up to raw abscissa s_l^1, i.e. that the values of $\hat{s}_f^1$, $\hat{s}_f^2$ and $\hat{s}_l^1$ are available. The objective at time t_2 is therefore to compute the local scale factor on the part $[\, s_l^1,\, s_l^2\,]$ of the reference trajectory, see Figure 10.

Relying on the measured scale factor evaluated at time t_2, it can immediately be written that:

$$\hat{s}_l^2 - \hat{s}_f^2 = \lambda_m\,(s_l^2 - s_f^2) \tag{6}$$

Then, the local scale factor λ on the part $[\, s_l^1,\, s_l^2\,]$ of the reference trajectory is defined as the coefficient to be applied on the interval $[\, s_l^1,\, s_l^2\,]$, in order to meet the metric inter-distance derived from the telemetric data (according to (6)):

$$\lambda_m\,(s_l^2 - s_f^2) = \lambda\,(s_l^2 - s_l^1) + \hat{s}_l^1 - \hat{s}_f^2 \tag{7}$$

Finally, if $T(u) = (\, T_x(u),\, T_y(u)\,)$ denotes the 2D-parametric equations of the reference trajectory T in the absolute frame $[A,\, X_A,\, Y_A)$ (see Figure 2), then the corrected curvilinear abscissa at any $s \in]\, s_l^1,\, s_l^2\,]$ can be computed according to:

$$\hat{s} = \hat{s}_l^1 + \int_{u_l^1}^{u_s} \lambda \left|\left| \frac{dT}{du}(u) \right|\right| du \tag{8}$$

where u_l^1 *(resp. u_s)* is the parameter value of 2D-curve $T(u)$ associated with the curvilinear abscissa s_l^1 *(resp. s)*.

C. Recorded local scale factor

According to (7), each coefficient λ is attached to a very small part of the reference trajectory T. In order to contain the computational burden when correcting vehicle curvilinear abscissas, these numerous parameters have to be gathered.

Since T is here described as a B-Spline curve, one local scale factor has been associated to one piece of the B-Spline. More precisely, if $T_k(u)$ (with $u \in [0,\, 1]$) denotes the k^{th} piece of the B-Spline T (with $k \in \{1,\, m\}$), then the recorded local scale factor $\lambda_{r,k}$ associated to $T_k(u)$ is defined as:

$$\lambda_{r,k} = \frac{\int_0^1 \lambda(u) \left|\left| \frac{dT_k}{du}(u) \right|\right| du}{\int_0^1 \left|\left| \frac{dT_k}{du}(u) \right|\right| du} \tag{9}$$

where $\lambda(u)$ is the constant-piecewise function constituted of the coefficients λ computed according to (7) along $T_k(u)$. Parameters $\lambda_{r,k}$ are computed on-line, as soon as the 2^{nd} vehicle leaves the k^{th} piece $T_k(u)$ of the reference trajectory.

The m factors $\lambda_{r,k}$ can also be stored, for subsequent uses, in a file attached to the reference trajectory T. Then, anytime the same trajectory is followed, accurate platoon control can be achieved solely from monocular vision, since the corrections to be applied to the visual virtual world are already available.

V. Experimental results

In order to investigate the capabilities of the proposed approach, preliminary experiments have been carried out with two vehicles at Campus des Cézeaux, in Clermont-Ferrand.

A. Experimental vehicles

The experimental vehicles are shown in Figure 1. They are electric vehicles, powered by lead-acid batteries providing 2 hours autonomy. Two *(resp. four)* passengers can travel aboard the Cycab *(resp. the RobuCab)*. Their small dimensions (length 1.90m, width 1.20m) and their maximum speed (5 $m.s^{-1}$) are appropriate to urban environments. Vehicle localization algorithms and platoon control laws are implemented in C++ language on Pentium based computers using RTAI-Linux OS.

Laser rangefinders provide telemetric data at a 60Hz sampling frequency, with a standard deviation within 2cm. The cameras supply visual data at a sampling frequency between 8 and 15Hz, according to the luminosity. The inter-vehicle communication is ensured via WiFi technology. Since the data of each vehicle are transmitted as soon as the localization step is completed, the communication frequency is similar to the camera one. Finally, each vehicle is also equipped with an RTK-GPS receiver, devoted exclusively to performance analysis: its information are not used to control the vehicles.

B. Experimentations

All the experiments reported below consist in platoon control, with two vehicles, along the 250m-long U-trajectory shown in Figures 5-6. The leading vehicle speed is 1 $m.s^{-1}$.

In the first experiment, raw curvilinear abscissa supplied by vision has been directly used into the longitudinal control law. The curvilinear inter-distance computed from these raw vision data and from RTK-GPS measurements are displayed respectively in red dashed line and black solid line in Figure 11.

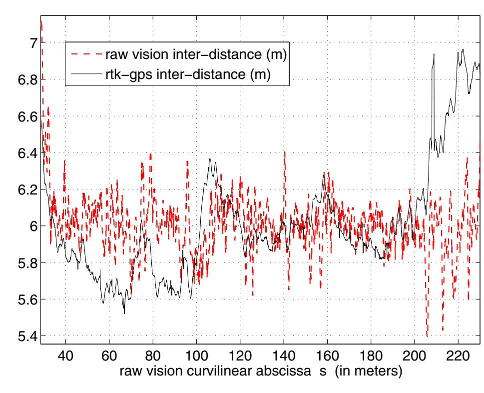

Fig. 11. Inter-distances when platooning is achieved from raw vision data

It can be noticed that the variable explicitly controlled, i.e. the curvilinear inter-distance computed from raw vision data, is kept close to the desired value $d = 6$m, as expected. However, RTK-GPS measurements reveal that on some parts of the trajectory, the actual inter-distance is far from this expected value: 5.6m at the beginning of the trajectory, and 6.8m at its end. The distorsions in the visual world affect significantly platooning accuracy, and lead to poor performances.

In the second experiment, the laser rangefinder of the 2^{nd} vehicle has been used to compute on-line the local scale factors λ, and longitudinal control has been achieved with the corrected curvilinear abscissa. The curvilinear inter-distance computed from these corrected vision data and from RTK-GPS measurements are displayed respectively in blue dashed line and black solid line in Figure 12.

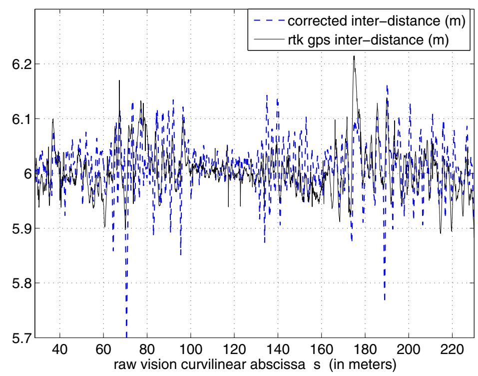

Fig. 12. Inter-distances when platooning is achieved from corrected data

It can be observed that the correction introduced on the raw vision data is definitely relevant, since the inter-distance supplied by corrected vision data is very close to the actual one provided by the RTK-GPS sensor. Consequently, platoon control is satisfactorily achieved: the longitudinal error is generally inferior to 10cm during this experiment.

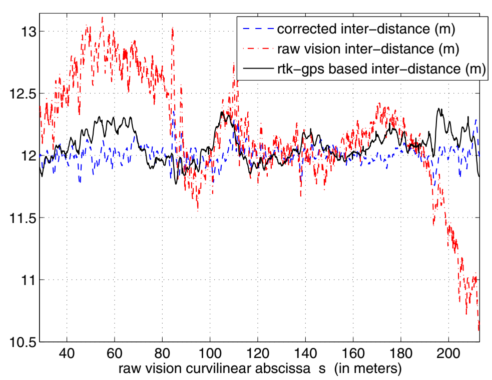

Fig. 13. Inter-distances when platooning is achieved from recorded $\lambda_{r,k}$

Finally, in order to demonstrate that not only the 2^{nd} vehicle, but any vehicle in the platoon, can be accurately controlled, the local scale factors $\lambda_{r,k}$ computed during the second experiment have been used in a third one, where the desired inter-distance was $d = 12$m. Vehicle localization was derived solely from vision data, corrected with the previously recorded $\lambda_{r,k}$. The curvilinear inter-distance computed from raw vision data, from corrected vision data and from RTK-GPS measurements are displayed respectively in red dot-dashed line, blue dashed line and black solid line in Figure 13.

First, it can be observed that platoon control is again satisfactorily achieved. Then, it can also be noticed that the curvilinear inter-distance computed from raw vision data is largely erroneous, and would have led to very large errors if reported into the control law. This establishes once more that accurate platoon control can be achieved only if vision data are previously corrected according to a set of local scale factors.

VI. Conclusion

In this paper, vehicle platooning in urban environments has been addressed. A global decentralized control strategy has been proposed, in order to avoid servoing error accumulation. Moreover, nonlinearities in vehicle models have been explicitly taken into account to enable high accurate guidance.

Absolute vehicle localization relies mainly on on-board cameras. However, since the visual virtual world is slightly distorted w.r.t. the actual metric one, a set of local scale factors has been derived from the laser rangefinder of the 2^{nd} vehicle to refine the localization of any vehicle in the platoon.

Preliminary full scale experiments, carried out with two vehicles, have demonstrated the efficiency of the proposed approach. Further experiments, involving several vehicles, in different urban environments and with different weather conditions have to be conducted. However, with respect to the two last points, the robustness of vision algorithms has already been demonstrated (e.g. [8] and [9]), so one may be quite confident.

References

[1] S. Benhimane and E. Malis. Vision-based control for car platooning using homography decomposition. In *Intern. Conf. Robotics & Automation (ICRA)*, pages 2173–2178, Barcelona (Spain), 2005.

[2] J. Bom, B. Thuilot, F. Marmoiton, and P. Martinet. A global strategy for urban vehicles platooning relying on nonlinear decoupling laws. In *Intern. Conf. Intelligent Robots Systems (IROS)*, pages 1995–2000, 2005.

[3] P. Daviet, S. Abdou, and M. Parent. Platooning for vehicles and automatic parking by scheduling robotic actions. In *Intern. Symposium Robotics and Manufacturing (WAC)*, Montpellier (France), 1996.

[4] A. De Luca, G. Oriolo, and C. Samson. Feedback control of a non-holonomic car-like robot. In *Robot Motion Planning and Control* J.P. Laumond ed - pages 171-253, vol 229 of LNCIS, Springer-Verlag, 1998.

[5] P. Evans. New energy sources for the car : how Toyota sees the future. *Energy News (Australian Institute of Energy)*, 18(2), June 2000.

[6] R. Horowitz and P. Varaiya. Control design of an automated highway system. *Proc. IEEE*, 88(7):913–925, July 2000.

[7] C. Laugier. Towards autonomous vehicles for future intelligent transportation systems. In *Conf. of Italian Association in Artificial Intelligence*, pages 251–258, Padova (Italy), 1998.

[8] E. Royer, J. Bom, M. Dhome, B. Thuilot, M. Lhuillier, and F. Marmoiton. Outdoor autonomous navigation using monocular vision. In *Intern. Conf. Intelligent Robots & Systems (IROS)*, pages 3395–3400, 2005.

[9] E. Royer, M. Lhuillier, M. Dhome, and T. Chateau. Localization in urban environments : monocular vision compared to a differential GPS sensor. In *Intern. Conf. Computer Vision & Pattern Recognition (CVPR)*, 2005.

[10] C. Samson. Control of chained systems. application to path following and time-varying point stabilization of mobile robots. *IEEE Transactions on Automatic Control*, 40(1):64–77, January 1995.

[11] S. Shaheen, K. Wipyewski, C. Rodier, L. Novick, M.A. Meyn, and J. Wright. Carlink II: a commuter carsharing pilot program final report. PATH Research Report, Univ. of California, Berkeley (USA), 2004.

[12] B. Thuilot, J. Bom, F. Marmoiton, and P. Martinet. Accurate automatic guidance of an urban electric vehicle relying on a kinematic GPS sensor. In *Intern. Symposium on Intelligent Autonomous Vehicles (IAV)*, 2004.

[13] D. Wang and M. Pham. Unified control design for autonomous car-like vehicle tracking maneuvers. In *Autonomous Mobile Robots: sensing, control decision-making, applications,* pages 295-329, CRC Press, 2006.